



A Thermal Analysis of a 1.5 Meter f/5 Fused Silica Primary Lens For Solar Telescopes

Peter G. Nelson
February 2007

ABSTRACT

A potentially important issue with using a large and fast refracting primary in a solar telescope is the thermal heating due to absorption of sunlight. We examine these effects for a 1.5 meter diameter lens made of fused silica with a focal ratio of f/5. Such a lens has a sagitta of ~70mm and a center thickness of ~150mm. Because glass is such a poor thermal conductor, even small amounts of absorbed power can cause heat to build up in the center of the lens's body. A careful analysis conducted for standard-grade Corning 7980 fused silica shows that the impact on image quality and polarization can be rendered negligible by simple means.

Methodology

A black-body radiation model was assumed for the solar spectrum, and this was normalized to produce 1.8 W/m²/nm of peak power at 500nm¹. Corning has provided the measured internal transmission for standard-grade 7980 fused silica over the wavelength range of 200nm to 4300nm (the total range over which fused silica is transmissive)². These data were combined with the solar spectrum to estimate the power absorbed at each wavelength (in 50nm bandwidth bins). Thermal models are very sensitive to where the power is absorbed. We assumed that the absorption of light in the bulk glass follows an exponential decay:

$$I(\lambda) = I_0(\lambda) \times \exp(-\alpha(\lambda)T) \quad [1]$$

where (I_0) is the incident intensity (W/m²), (α) is the absorption coefficient, (T) is the thickness of the glass traversed in cm, and (I) is the final intensity after traversing that thickness. The coefficient α was calculated for each wavelength from 200nm to 4300nm in 50nm steps from the Corning transmission data. The ~0.5% of solar radiation above 4300nm was assumed to be completely absorbed in the 1st cm of glass.

To model the spatial power distribution, the lens was broken up into 15 1-cm layers (shown in Figure 1 below). Given the intensity of incident radiation and the absorption coefficient, it is possible to calculate how much power is deposited in each layer *for each of the 83 wavelength*

bins from 200-4300nm. The contribution from each wavelength was summed for each layer, and this gave the power total dissipated in each layer.

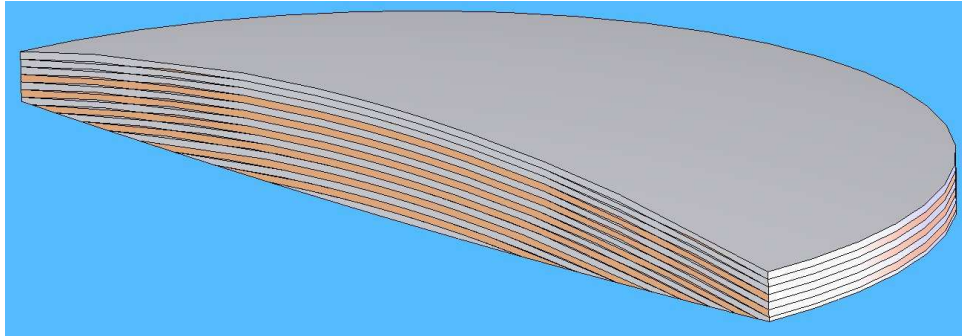


Figure 1: The layered lens. The alternating colors are only a visual aid to identify the layers. The top surface in the figure is facing the Sun.

The power dissipation for each layer was then entered into a Finite Element Analysis (FEA) model for the optic. Assumptions were made for the radiative, convective, and fixed boundary conditions, from which the steady-state temperature distribution was calculated.

The absorption data

Table 1 below tabulates the absorption data from Corning and shows the calculated power dissipation for the first cm of glass (the far right column). The absorption values (%/cm) were read from graphs provided by Corning. To calculate the total power absorbed in the first layer, the entire right-hand column in the table was summed. The calculation of absorbed power was repeated for each consecutive 1-cm layer of the lens.

Table 1: The absorption in standard grade Corning 7980 fused silica as a function of wavelength

Wavelength λ	% absorption/cm for fused silica	Calculated $\alpha(\lambda)$ (1/cm)	Model for $I_0(\lambda)$ in W/m^2 (50nm bw)	Power absorbed in first cm of glass / m^2
200	2	0.0202	4.8862	0.0977
250	0.5	0.0050	19.4070	0.0970
300	0.25	0.0025	41.1609	0.1029
350	0.1	0.0010	62.5110	0.0625
400	0	0.0000	78.2474	0.0000
450	0	0.0000	87.0036	0.0000
500	0.05	0.0005	89.7010	0.0449
550	0.075	0.0008	88.0136	0.0660
600	0.08	0.0008	83.5493	0.0668
650	0.08	0.0008	77.5628	0.0621
700	0.1	0.0010	70.9289	0.0709
750	0.1	0.0010	64.2108	0.0642
800	0.1	0.0010	57.7449	0.0577
850	0.1	0.0010	51.7135	0.0517
900	0.1	0.0010	46.1999	0.0462
950	0.35	0.0035	41.2263	0.1443
1000	0.1	0.0010	36.7789	0.0368
1050	0.12	0.0012	32.8249	0.0394
1100	0.13	0.0013	29.3221	0.0381
1150	0.15	0.0015	26.2256	0.0393
1200	0.18	0.0018	23.4908	0.0423
1250	0.75	0.0075	21.0760	0.1581
1300	0.3	0.0030	18.9428	0.0568
1350	1.3	0.0131	17.0568	0.2217
1400	12	0.1278	15.3875	1.8465

1450	0.6	0.0060	13.9079	0.0834
1500	0.25	0.0025	12.5944	0.0315
1550	0.5	0.0050	11.4264	0.0571
1600	0.5	0.0050	10.3861	0.0519
1650	0.5	0.0050	9.4577	0.0473
1700	0.5	0.0050	8.6277	0.0431
1750	0.5	0.0050	7.8843	0.0394
1800	0.75	0.0075	7.2174	0.0541
1850	1	0.0101	6.6178	0.0662
1900	1	0.0101	6.0779	0.0608
1950	1	0.0101	5.5909	0.0559
2000	1	0.0101	5.1507	0.0515
2050	2	0.0202	4.7523	0.0950
2100	2.5	0.0253	4.3910	0.1098
2150	5	0.0513	4.0629	0.2031
2200	40	0.5108	3.7644	1.5058
2250	25	0.2877	3.4925	0.8731
2300	10	0.1054	3.2443	0.3244
2350	5	0.0513	3.0176	0.1509
2400	5	0.0513	2.8100	0.1405
2450	12	0.1278	2.6198	0.3144
2500	20	0.2231	2.4453	0.4891
2550	35	0.4308	2.2849	0.7997
2600	55	0.7985	2.1373	1.1755
2650	80	1.6094	2.0014	1.6011
2700	99.9	6.9078	1.8760	1.8741
2750	99.9	6.9078	1.7601	1.7584
2800	99.9	6.9078	1.6530	1.6514
2850	85	1.8971	1.5539	1.3208
2900	60	0.9163	1.4620	0.8772
2950	40	0.5108	1.3768	0.5507
3000	30	0.3567	1.2976	0.3893
3050	20	0.2231	1.2241	0.2448
3100	17	0.1863	1.1556	0.1965
3150	15	0.1625	1.0918	0.1638
3200	12	0.1278	1.0323	0.1239
3250	10	0.1054	0.9769	0.0977
3300	8	0.0834	0.9250	0.0740
3350	8	0.0834	0.8766	0.0701
3400	10	0.1054	0.8312	0.0831
3450	15	0.1625	0.7888	0.1183
3500	30	0.3567	0.7490	0.2247
3550	40	0.5108	0.7116	0.2846
3600	50	0.6931	0.6766	0.3383
3650	60	0.9163	0.6437	0.3862
3700	75	1.3863	0.6127	0.4595
3750	80	1.6094	0.5836	0.4669
3800	80	1.6094	0.5562	0.4449
3850	80	1.6094	0.5303	0.4243
3900	80	1.6094	0.5060	0.4048
3950	83	1.7720	0.4830	0.4009
4000	85	1.8971	0.4613	0.3921
4050	90	2.3026	0.4408	0.3967
4100	95	2.9957	0.4214	0.4004
4150	96	3.2189	0.4031	0.3870
4200	98	3.9120	0.3858	0.3780
4250	98	3.9120	0.3693	0.3620
4300	99.9	6.9078	0.3538	0.3534
Total Power in W/m²			1359.90	28.04

Table 2 below shows the result of summing over the power contributions from each wavelength bin in each layer. This was combined with each layer's area to estimate the total power dissipated per layer. Note that the bottom 8 layers of the lens have very tapered edges. The

areas shown in the table represent the *top* area of the layer, so the calculated absorption is an overestimate. Summing over all layers, the total power dissipation for light from 200nm to 4300nm is 159.4W. Because fused silica becomes totally opaque above ~4300nm, we added an additional 11W to the power absorbed in layer 1 (representing the ~0.5% of solar radiation above the 4300nm). This is an overestimate since it doesn't consider IR absorption in the atmosphere.

Table 2: A summary of power absorption calculated for each layer of the lens.

Layer:	1	2	3	4	5	6	7	8
W/m ² in layer	28.04	11.97	8.75	7.16	6.18	5.49	4.97	4.58
Layer area (m ²)	1.78	1.78	1.78	1.78	1.78	1.78	1.78	1.69
Total W/layer	49.91	21.31	15.58	12.75	10.99	9.77	8.86	7.74
Layer:	9	10	11	12	13	14	15	
W/m ² in layer	4.26	4.00	3.78	3.59	3.43	3.29	3.17	
Layer area (m ²)	1.47	1.26	1.05	0.84	0.63	0.42	0.21	
Total W/layer	6.26	5.04	3.97	3.02	2.16	1.38	0.67	
Total Power	-----							159.39

FEA modeling

The solid model shown in Figure 1 was composed using SolidWorks™ which directly integrates COSMOS™ finite element analysis software from Structural Research & Analysis Corp. The version used for this analysis can analyze thermal models where boundary conditions include heating or cooling power applied to a volume or surface, fixed temperatures, radiative cooling and heating from a surface, and convection. The convective model does not use computational fluid dynamics (CFD), but allows you to assign a convection coefficient in W/m²K to a surface. For this study, it was assumed that the ambient temperature was 20°C.³ The model used in this study had over 37,000 elements evenly distributed throughout the layers.

The heating powers tabulated in Table 2 were distributed uniformly throughout the volume of each layer in the model. The edges of the lens were assumed to be thermally controlled by the lens cell at 0.75°C above ambient (20.75°C). This elevated temperature was determined iteratively from the FEA to give a smooth temperature gradient near the edge of the lens (Figure 2 and Figure 3). This reduces both the thermal gradient and internal stress. The front and rear surfaces were allowed to radiate into the environment. Glass has a near-perfect emissivity which typically ranges between 0.91-0.94⁴. For this study we assumed the conservative value of 0.9. For radiative cooling, one must also define the ambient temperature and a “view factor” which (roughly) defines the fraction of the 2π half-solid angle seen by the radiating surface. For both surfaces we assumed a view factor of 90% and an ambient temperature of 20°C. Finally, we assigned a convective cooling coefficient for both the front and rear surfaces. The rear surface of the lens is exposed to the sealed telescope tube, which is filled with He. This gas is not circulated for contamination reasons, but it is also not required; as Table 2 shows, the vast majority of the heat is absorbed in the front few cm of the lens. Passive convective cooling with air is usually in the range of 5-25 W/m²K.⁴ Helium is a much better thermal conductor, so we assume a value of 30 W/m²K. The front surface of the lens is exposed to a constant and high-volume stream of HEPA filtered air (to reduce particulate contamination). Forced-air cooling has a much higher convection coefficient which ranges from 20 to 300 W/m²K.⁴ We assumed a value of 100 W/m²K. With the boundary conditions defined, the FEA software can calculate the temperature evolution in the lens:

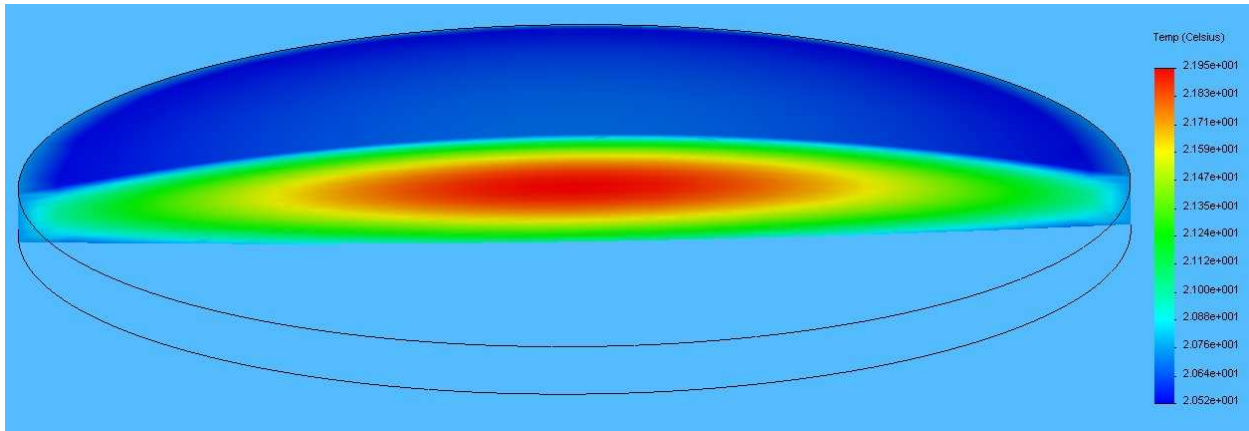


Figure 2: A map of the internal temperature profile of the lens in the steady-state case. The temperature range (blue to red) is 20.0 - 21.6 °C.

A time-evolution analysis shows that the core temperature of the lens rises by 0.5°C within half an hour of exposure to the Sun. Within two hours the temperature stabilizes within 2% of the steady-state distribution. The peak core temperature is ~2°C above ambient.

The analysis was repeated with a convection coefficient of 20 W/m²K for the front surface of the lens (the lowest expected value for forced convection cooling). In this case, the peak core temperature increased by ~60% (to 3.13°C above ambient). This reflects the fact that the cooling is dominated by the (poor) thermal conductivity of the glass.

Optical analysis

There are three ways in which heating affects the primary lens. First, the index of refraction has a temperature coefficient which can cause a radial gradient in the index. This index variation can change the effective focal length and introduce distortion. Secondly, the increase in core temperature distorts the figure of the optic through its coefficient of thermal expansion (CTE). Lastly, the temperature gradients induce stress into the glass which can cause birefringence. This is very important to consider for COSMO, which seeks to make very high-precision polarization measurements.

Many of the FEA techniques used here are described in detail in other COMSO Technical Notes.⁵ Briefly, the FEA model is capable of exporting temperature, deformation, and stress data to text-formatted data files. MatLab is used to read these files and perform a variety of analyses. Of particular interest is the ability of MatLab to interface directly with ZEMAX optical modeling software using the “MZDDE ZEMAX toolbox” produced by Defencetek/CSIR. ZEMAX is capable of modeling index gradient lenses as well as distorted surfaces using their “Gradient” and “Extended Polynomial” surface types. The details of the birefringence analysis are very involved, and reader is referred to the reference cited above.

Index variations

A wavefront can be bent in an optic by horizontal gradients in the index of refraction. Light deflection by gradients in the axial direction is a higher-order effect and is ignored. The 3-D temperature profile shown in Figure 2 was averaged first through the thickness of the lens and

then over the azimuth angle. The results are shown in Figure 3. The scatter in the data points simply reflects the fact that elements in the FEA model are not perfectly distributed throughout the solid model. A least-squares fit of a 12th order even polynomial in radius is shown in red. This is multiplied by fused silica’s index of refraction (1.45) and the temperature coefficient of the index (9.5934 ppm/°K) at 1075nm⁶. The result is the net index variation as a function of radius, which is shown in Figure 4.

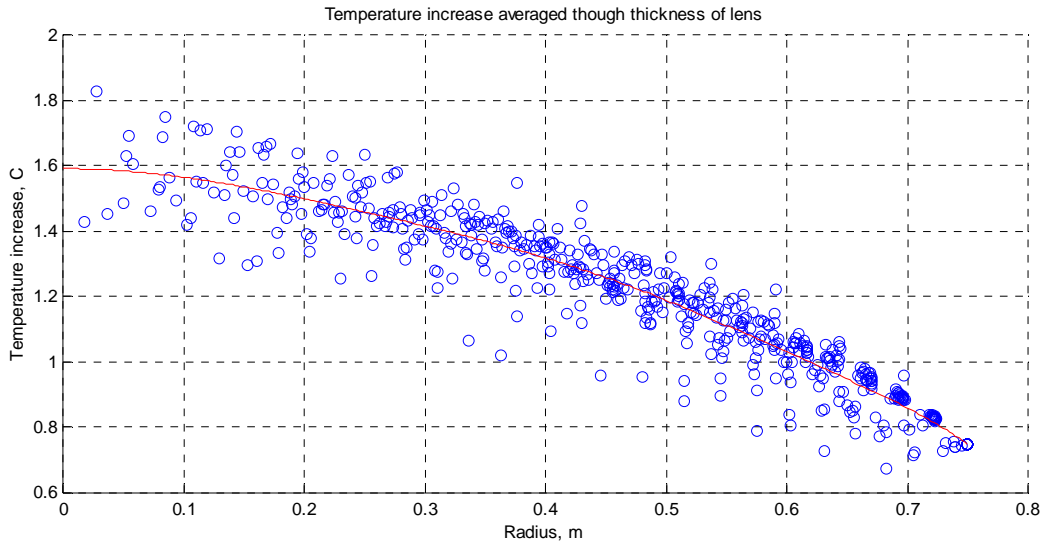


Figure 3: The temperature averaged through the thickness of the lens. Each blue circle represents the average of 100 elements at a given radius (there are 37,000 elements in the model). The red line is a polynomial fit to these data.

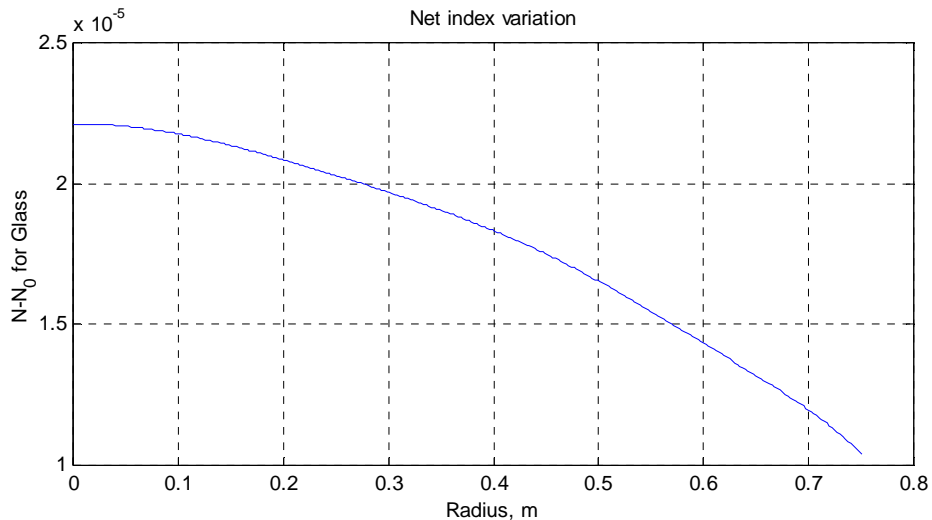


Figure 4: The index variation over the radius of the lens.

This index gradient (in polynomial form) is imported by ZEMAX into a “Gradient 2” surface. Unfortunately, ZEMAX does not have the capability to model an aspheric optic with an index gradient. To solve this problem, the geometry shown in Figure 5 is used. It replaces the nominal aspherical COSMO primary with a ‘best-fit’ spherical optic (of “Gradient 2” type) followed by

an aspherical corrector. The ‘best fit’ spherical optic differs from the true optic by no more than 150 microns, so the effects of the index gradient should be very accurately represented. Though the spot diagram formed by the two-optic system is significantly different from the COSMO singlet (see Figure 8a), it is perfectly adequate for evaluating the magnitude of the effect.

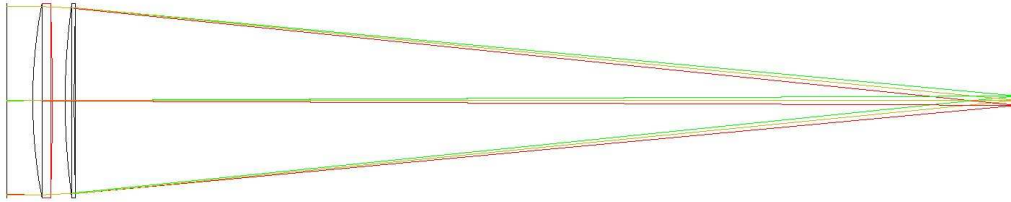


Figure 5: The ZEMAX model used for index variations. A ‘best-fit’ spherical optic is used instead of the nominal aspherical COSMO lens. A second aspherical lens is used to correct the aberrations and form a high-quality spot diagram.

Figure 6 below shows the spot diagrams before and after the index gradient was applied to the lens. All spot diagrams are shown with the Airy disk for an absolute reference. The RMS size of the spot increases from 5.9microns to 6.4 microns, or a little less than 10%. The first FEA studies held the lens cell temperature (the lens’s edges) at the ambient 20°C. This resulted in a significant extension of the horizontal ‘wings’ in Figure 6b, and an RMS size of over 7 microns. The optimal temperature for the lens cell may require some experimentation.

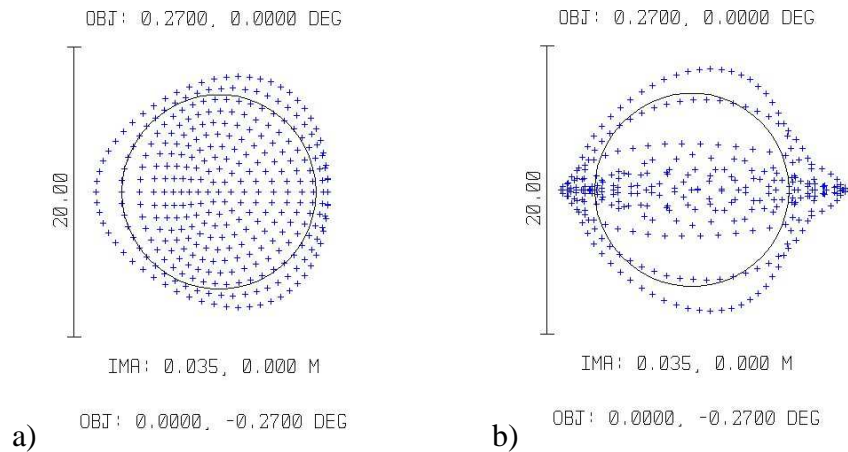


Figure 6: The spot diagram for a) the system at a uniform temperature and b) with the temperature-induced radial index variation. Note the focus was *not* adjusted after the index variation was applied.

Deformation of the figure

The FEA software is capable of taking the temperature profile calculated from the thermal study and using it as an input to a mechanical deformation study. The deformation is primarily driven by the coefficient of thermal expansion, which is 0.57 ppm/°K for Corning’s 7980 fused silica. As Figure 7 shows, the deformation is very uniform and spherical in character. The peak deformation is at the top center of the lens, which deforms by 0.23microns outward. The bottom surface sees a much smaller displacement: only 0.029microns. The difference is due to the fact that the lens has a very large sag, which puts a lot of material in ‘front’ of where it is held at its edges. Most of heat is also deposited in the front half of the lens.

As was done for the gravitational deformation study of COSMO Technical Note #2,⁵ the deformation data were exported to a file and fit by a 4th order, 2-D polynomial in MatLab. This polynomial was exported to ZEMAX, and the resulting spot diagrams calculated. These are shown in Figure 8 below.

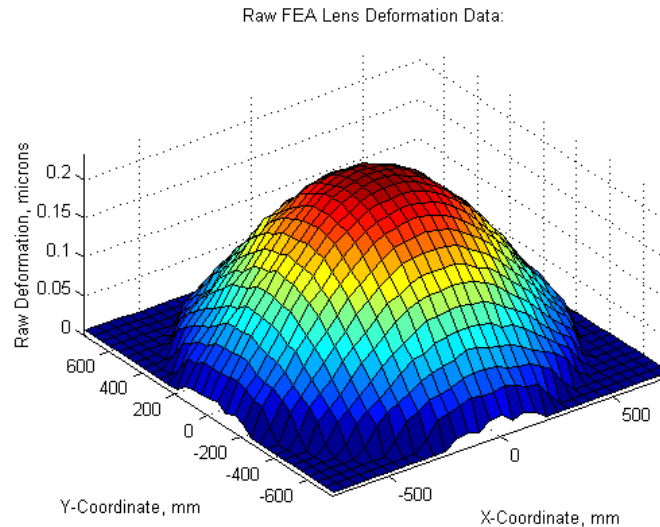


Figure 7: The raw FEA deformation data for the top surface of the lens.

As can be seen, the change in the spot diagram is again very small. The RMS radius of the normal spot diagram (Figure 8a) is 7.1microns. The RMS radius of the spot for the deformed lens is only 7.5 microns; only a 6% change.

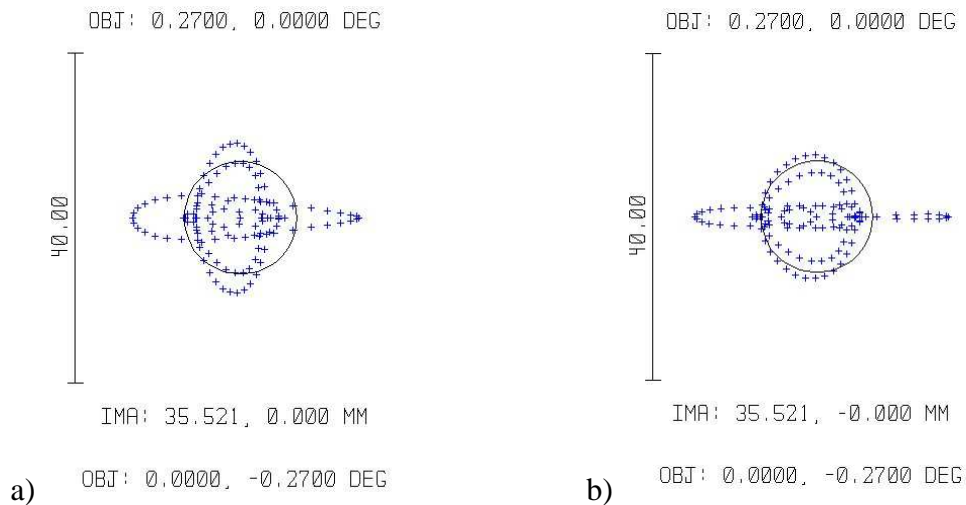


Figure 8: The spot diagrams for a) the system before deformation and b) with the front and rear surface figures of the lens deformed by the expansion of the lens's core.

Stress-induced birefringence

In addition to the deformation data, the FEA calculation also produced a 6-component stress tensor for each of the 37,000 elements in the lens. It can be shown⁵ that three of these can be neglected, and only the in-plane components considered (the normal X and Y strains, plus the

shear in the X-Y plane). From these data, the birefringence at each point in the lens can be calculated and averaged through the thickness of the lens. The results from this analysis are shown in Figure 9 below.

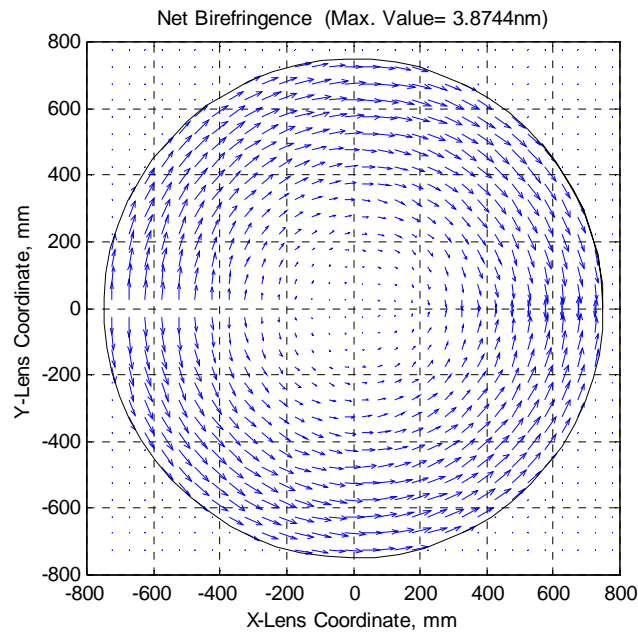


Figure 9: A map of the birefringence in the lens. The direction of the arrows shows the axis of birefringence (note that there is a 180° ambiguity in the arrows' directions). The length of the arrows show the magnitude.

As expected, there is perfect symmetry about the axis of the lens, reflecting the azimuthal symmetry of the light's heating. It is also possible to calculate the Mueller matrix from the stress components:

1.000	0	0	0
0	1.000	-5.8079e-012	1.2906e-006
0	-5.8079e-012	1.000	9.0000e-006
0	-1.2906e-006	-9.0000e-006	1.000

Table 3: The Mueller matrix representing the polarization transfer function for the heated lens.

The very low values of the off-diagonal matrix elements also show the extreme symmetry of the geometry. In principle, all these values should be exactly zero. Their finite values are a result of numerical errors in the simulation, and finite-sampling effects.

If the lens is not uniformly illuminated, there could be a more significant net birefringence. It is important to note that the peak value shown in Figure 9 is only 3.9nm. This should be compared with the birefringence of the blank itself, which is rated at less than 1nm/cm (data from Corning for a full-sized fused-silica boule)⁷. The edge of the lens is ~7cm thick, and the center of the lens is 15cm thick, which correspond to a maximum of 7 and 15 nm of birefringence respectively. Thus, while 3.9nm is not very small in comparison, it is clearly not a dominant effect either.

Conclusions

Three different thermal effects were considered in this analysis, and none proved to be significant. This is due largely to the remarkable properties of fused silica, which has been refined to extraordinary levels by the telecommunications industry. Chief among these properties is the very low level of absorption of energy over the solar spectrum. This more than offsets the larger-than-average dn/dt of fused silica.

The study also found most of the power is absorbed in the first few cm of the lens. This is fortunate since the high-volume HEPA air-washing system of COSMO provides a large amount of cooling power to the front surface, and removes most of this heat.

The results of this study came from a 'zero-atmosphere' model for the solar light. Thus all results should be scaled (at least) for the peak intensity at the observatory's site (to be determined). No compensation was made for the absorption bands in the atmosphere, which could significantly reduce the power at some of the fused silica absorption bands (caused primarily by OH ions). In the end, none of this is necessary, since no significant effects were found in the calculation. It will certainly be prudent to carefully control the lens cell's temperature. Also, since there is a long tubular 'snorkel' extending from the end of the COSMO telescope (for clean-air flushing) the telescope tracking should be good before opening the telescope shutter. This will prevent differential heating of the lens due to shadowing of the snorkel, and keep the net birefringence of the lens low.

¹ This is actually an above-atmosphere value. The calculation ignores any absorption of the atmosphere, and therefore represents a very conservative assumption.

² The absorption data were measured in multiple historical samples.

³ The choice of ambient temperature only weakly affects the coefficient of thermal expansion, but otherwise does not change the results of the analysis.

⁴ These values come from the COSMOS FEA software documentation and material library.

⁵ See P.G. Nelson, "A Finite Element Analysis of Meter-Class Refracting Primary Objectives for Coronal Polarimetry," COSMO Technical Note No. 2

⁶ 1075nm is the wavelength of the FeXII coronal emission lines, and is the primary wavelength of interest for COSMO.

⁷ Corning points out that in large pieces of glass, stress related to finishing and fixturing can adversely affect the birefringence. Stress from the lens cell in COSMO has been evaluated in ref. (5) above, and found to be acceptable. Stress induced from finishing has not been evaluated, but is expected to be small.